Reinforcement of Elastomers ☆

CM Roland, Naval Research Laboratory, Washington, DC, USA

1 Types of Fillers

Employed as a pigment in Egyptian pottery dating to 4000 BC, carbon black is the pre-eminent reinforcing filler, able to impart a broad spectrum of properties to rubber compounds. There are over 40 grades of carbon black, with representative types listed in Table 1 (Hess and McDonald, 1983). Carbon black consists of solid, colloidal (<1 μm) entities called *aggregates*. Each aggregate is comprised of many primary particles fused together in a randomly arranged cluster, having a morphology akin to a bunch of grapes. The aggregate size and specific surface area are obviously important to rubber reinforcement, as are the number and arrangement of the particles within the aggregates. The latter govern the 'structure' of a given carbon black, which is a measure of the ratio of the effective volume of the aggregate to the sum of the primary particle volumes. Surface area can be measured by adsorption of a gas or an aqueous solution of surfactant (typically cetyltrimethylammonium bromide). The advantage of a fluid is that it is not absorbed in the angstrom–sized micropores of the aggregate that are likewise not accessed by polymer chains. Another common measure of surface area is the absorption of iodine, but although the method is very easy, the accuracy is poor, the results being affected by the surface chemistry of the filler (Donnet *et al.*, 2006). Structure is assessed from measurement of the internal void volume, usually by absorption of dibutyl phthalate, either on the carbon black as received ('DBPA') or after crushing and sieving the carbon particles ('CDBP' – crushed dibutyl phthalate). The surface area and structure of the particles determine how much rubber is 'immobilized' by the filler. The surface of carbon black is imperfect graphitic layers, with the carbon atoms at exposed edges containing $C=O$ and $C-OH$ groups, in the form of quinones, phenols, carboxyls, ketones, etc. Heating carbon black to high temperature (≥ 2700 °C) in an inert atmosphere removes the oxygen and hydrogen; polymer chains do not react with or chemisorb to such 'graphitized' carbon black.

Table 1 Characteristics of typical carbon blacks

ASTM type	Generic name	Particle size (nm)	Aggregate size (nm)	Surface area ($m^2 g^{-1}$)
N110	SAF	17 ± 7	54 ± 26	143
N220	ISAF	21 ± 9	65 ± 30	117
N330	HAF	31 ± 13	86 ± 44	80
N339	–	26 ± 11	75 ± 34	90
N351	–	31 ± 14	89 ± 47	75
N550	FEF	53 ± 28	139 ± 71	41
N660	GPF	63 ± 36	145 ± 74	34
N762	SRF	110 ± 53	188 ± 102	21
N990	MT	246 ± 118	376 ± 152	9

Colloidal silica is an alternative to carbon black, although typically the polarity difference between silica and common rubbers gives deficient reinforcing properties unless coupling agents are employed. Potential advantages of silica over carbon black include lower rolling resistance and reduced abrasive wear. Fumed silica is produced in a flame. Its aggregates tend to be less tightly clustered than those of carbon black, with silanol and nonpolar siloxane groups present on the surface. The main use for fumed silica is to reinforce silicone rubber, since its cost precludes more general application to rubbers.

The more common form of silica in the rubber industry is precipitated silica, formed by acidification of a sodium silicate solution (the same method used to form silica gel). Similar to carbon black, precipitated silica exists as aggregates, but unlike fumed silica, these aggregates tend to be more highly clustered, with some having the appearance of fragments of silica gel. The surface is covered with silanol groups, through which the aggregates bond to each other, as well absorb moisture. Achieving the reinforcing performance of carbon black with precipitated silica is problematic due to the different surface chemistry and morphology. Generally, in comparison to carbon black, silica has stronger particle-particle interactions, but weaker interactions with the rubber. Excellent properties have been obtained in tire compounds with precipitated silicas by improving the bonding to rubber, either by 'activating' the silica or by the addition of coupling agents to the compound (Brinke *et al.*, 2003).

A method that circumvents the problem of dispersing silica in rubber is by *in situ* precipitation, for example, via catalyzed hydrolysis of tetraethoxysilane. Small (<25 nm), irregularly shaped particles can be obtained, with both the particle size and degree of aggregation controlled by the precipitation and processing conditions. Although the method may have potential for industrial operations such as reactive extrusion processing, there is no industrial-scale application of this approach to date.

Other inorganic particulates, including kaolin clay and calcium carbonate, have found use in the industry, and as mentioned, zinc oxide was the first reinforcing filler for rubber. Since mineral fillers are cheaper than the polymer, they serve as low-cost extenders, while also increasing the modulus; however, they do not provide high degrees of compound reinforcement. As discussed in Section 5, the failure properties of mineral-filled compounds are poorer than rubber containing carbon black.

Short fibers, including glass, cellulose, carbon, and aramid, are used to a limited extent in rubber, generally in combination with carbon black or silica. They increase the modulus and dimensional stability of rubber components, and given their large aspect ratio, can potentially yield anisotropic properties. Generally the fibers must be coated to facilitate dispersion and enable bonding to the elastomer.

A more recent development is the use of organo-modified, layered mineral silicates (clay). The material is relatively low cost and has been studied as a reinforcing filler in many polymers. Property improvements require intercalation, whereby polymer chains diffuse into the layer galleries, or exfoliation, in which there is separation of the silicate layers to yield nm-thick disks dispersed in the polymer. This 'nanoclay' is a two-dimensional filler, similar to graphene. The state of dispersion of the nanoclay can be deduced from X-ray measurements of the silicate d-spacing (lack of a diffraction peak indicating exfoliation). Although the performance enhancements and relatively low cost of organo-modified clays are attractive, inducing intercalation or exfoliation is a formidable problem, especially for non-polar polymers.

Dispersion is a general issue with the utilization of nano-particles. Carbon nanotubes, graphene, nano-diamond, as well as the modified silicates, have all shown the potential to yield enhanced properties, and a significant amount of research has been directed toward their application to rubbery materials (Feldman, 2012; Bokobza, 2013; Alateyah *et al.*, 2013; Sadasivuni *et al.*, 2014; Shakun *et al.*, 2014). However, the high surface areas and large surface energies promote particle agglomeration. Laboratory studies rely on dispersion methods involving solvents, sonication, freeze-drying, chemical treatments, etc., none of which are especially amenable to economical scale-up. The key to exploiting nano-fillers in the rubber industry is overcoming this dispersion problem.

2   Mixing and Dispersion

Reinforcement requires good dispersion of the filler, which is accomplished on an industrial scale by mixing in an internal mixer or two-roll mill. This mixing is energy-intensive and has the potential to degrade the compound by chain-scission or premature curing. During mixing the filler aggregates become uniformly distributed (on a scale of tens to hundreds of microns), the polymer is incorporated into the void spaces of the agglomerated pellets, and ultimately (the most difficult step) the filler agglomerates are broken down into distinct aggregates. At the usual filler concentrations (volume fraction 10–20%), the dispersed aggregates have some contact with each other, even when well distributed. These contacts may increase after mixing, driven by enthalpic particle interactions; this is undesirable because it increases the mechanical hysteresis of the elastomer (Section 4). Sufficient interaggregate contacts give rise to a filler network (Section 3.3), which is manifested in an elevated dynamic modulus at low strains and, at least for carbon black, high electrical conductivity. Reagglomeration and network formation can be a particular issue with silica, causing hardening of the rubber prior to curing.

Dispersion of filler is important to minimize hysteresis (Section 4) and, since particles larger than the intrinsic flaw size, which is on the order of 10–30 μm (Choi and Roland, 1996), can act as defects, very poor dispersion can affect failure properties. The complexity of the structure of carbon black, silica, etc. implies there are different degrees of dispersion. Conventional mechanical mixing does not fracture the aggregates, although some reduction in structure may occur. The term 'dispersion' refers to the
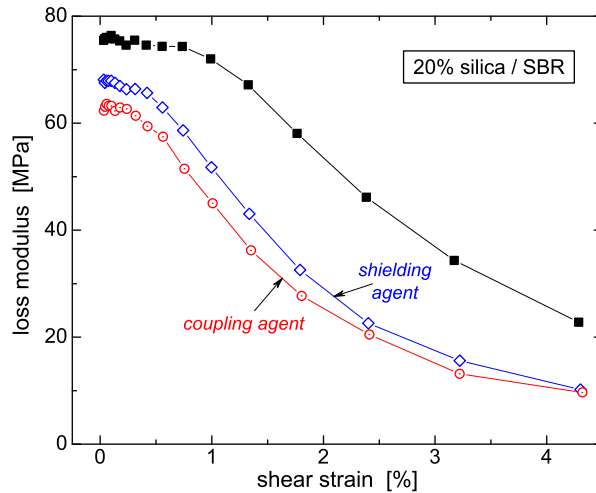
Figure 1   Dynamic loss modulus as a function of shear strain for SBR reinforced with 20% by volume silica: untreated (squares); with 6.5% by weight *n*-octyltriethoxysilane shielding agent (diamonds); or 4.7% by weight 3-mercaptopropyltrimethoxysilane coupling agent (circles). Suppression of agglomeration reduces the hysteresis (Robertson *et al.*, 2011).
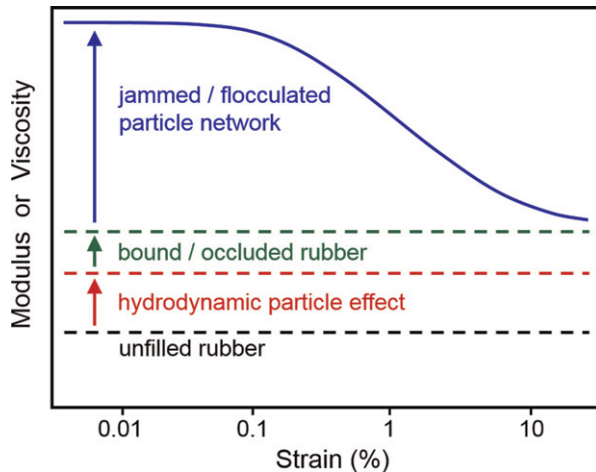
Figure 2   Schematic depicting the various contributions to the modulus and viscosity of rubber.

breakup of agglomerates or pellets, leading to separation and uniform distribution of the aggregates within the polymer. Optical microscopy or surface roughness measurements reveal agglomerates more than roughly 2 µm in size. A finer level of dispersion is reflected in a reduced Payne effect (Section 3.3) and for carbon black compounds, higher electrical resistivity.

    In addition to relying on adequate mechanical mixing to disperse the filler, polymers have been developed in which the chain-ends are terminated with reactive moieties that bond to the carbon black to inhibit particle agglomeration (Ulmer *et al.*, 1998). Also, coupling agents can be added to the rubber formulation for the same purpose. **Figure 1** shows dynamic mechanical loss measurements for a silica-reinforced styrene-butadiene copolymer (Robertson *et al.*, 2011). Reduction of the particle-particle interaction, and hence less energy dissipation, is achieved with either coupling or shielding agents, the latter reacting with the particle surface to suppress agglomeration.

3   Rheology and Modulus of Filled Rubber

There are various mechanisms underlying the effect of particulates on the deformation and flow of rubber. As illustrated in **Figure 2**, these include a hydrodynamic effect that amplifies the strain in the polymer phase; the occlusion of polymer chains within the void structure of the particles, enhancing their effective concentration; and a filler network structure when the amount of particles exceeds their percolation threshold. We consider each of these contributions in turn.

3.1   Hydrodynamic Effect

Particulate fillers increase both the viscosity and elastic modulus of a polymer or rubber compound via a hydrodynamic effect – the inextensible particles cannot deform, so their strain is transferred to the polymer chains. This strain-amplification is described by an extension of the Einstein viscosity equation for dilute, spherical particles, to account for particle interactions at higher concentrations (Guth, 1945):

$$\eta = \eta_0(1 + 2.5\phi + 14.1\phi^2)$$
$$G' = G'_0(1 + 2.5\phi + 14.1\phi^2) \tag{1}$$

In eqn [1] ϕ is the volume fraction of the filler, η and G' are the respective viscosity and dynamic storage modulus, and the subscript zero refers to the gum (unfilled) compound. Equation [1] is applicable, for example, to rubber filled with N990, a low surface area, low structure carbon black. However, for more reinforcing fillers, a significant amount of rubber becomes occluded within the void space of the aggregates (Section 3.2). This occluded polymer, which amplifies the hydrodynamic interaction, can be accounted for by including it in ϕ; that is, the magnitude of ϕ represents an effective volume fraction of filler (Medalia, 1973).

Non-spherical particles require a further modification of eqn [1]; a common expression for rodlike filler particles is the Guth–Gold equation (Guth, 1945):

$$\eta = \eta_0(1 + 0.67f\phi + 1.62f^2\phi^2) \tag{2}$$

which can also applied to the dynamic modulus. The aspect ratio of the rods is f; but for particles that are not rod-shaped, this parameter can be adjusted to fit the experimental data, yielding an effective shape factor (which underestimates the actual value).

In **Figure 3** (lower panel) are the viscosities for a polytetramethylene oxide with varying concentrations of multiwall carbon nanotubes (Casalini et al., 2012). Fitting eqn [2] to these data yields $f = 21$ for the particle aspect ratio. This is much less than the value for a single nanotube, indicating agglomeration. As shown in Section 3.3, this conclusion can be tested by analysis of the percolation threshold of the material, since the overlap concentration for the filler also depends on f (eqn [3]).

3.2   Rubber–Filler Interaction

Polymer chains will attach to reinforcing filler particles, especially carbon black, via chemisorption, or even covalent bonding if the filler has reactive sites. The term 'bound rubber' refers to chains bonded to the particles sufficiently strongly to resist dissolution in
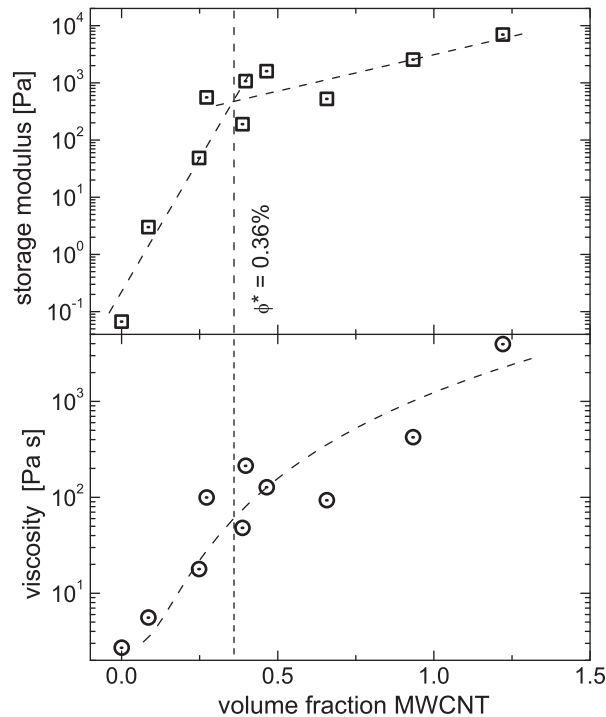
Figure 3   (Lower) Viscosity of PTMO as a function of filler content; the fitted line is the Guth–Gold equation with $f = 21$. (Upper) Storage modulus of the same compound, with the change in slope at a value of ϕ for which the percolation equation (eqn [3]) gives $f = 16$ (Casalini et al., 2012).
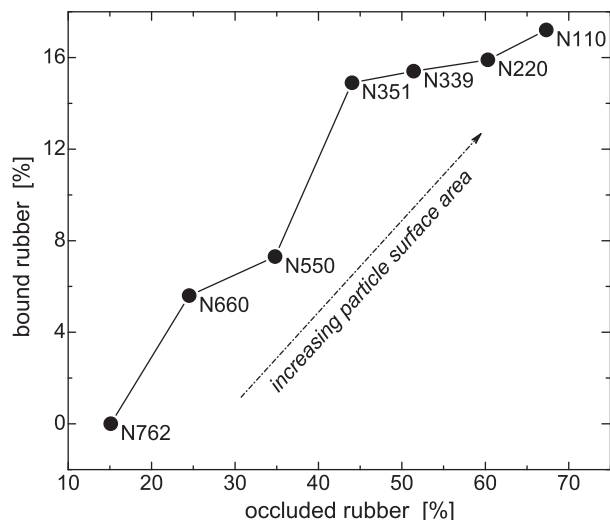
Figure 4 Quantity of rubber bonded to the filler versus the amount of rubber occluded in the particle structure for a 1,4-polybutadiene with 18% by volume carbon black of the indicated type (Robertson *et al.*, 2007).

a solvent. The amount of bound rubber generally correlates with the occluded rubber, as governed by the particle's surface area and structure (**Figure 4**) (Robertson *et al.*, 2007).

Precipitated silica gives considerably less bound rubber than a carbon black of similar surface area, and graphitized carbon black, in which surface imperfections and layer edges have been reduced by heating, yields negligible bound rubber.

The tethering of chains to the particle surface of the chains is expected to cause reduced mobility within the bound layer. It is for this reason that ϕ in eqn [1] underestimates the hydrodynamic effect, unless occluded rubber is included. However, this restriction on the mobility is limited. The occluded layer does not lose configurational freedom or become glassy (Robertson and Roland, 2008). The local segmental dynamics, encompassing correlated rotation of several backbone bonds, is usually unaffected by the presence of reinforcing filler.

3.3 Filler–Filler Interaction (Particle Network Formation)

The third mechanism for modulus enhancement of reinforced rubber is formation of a network of filler particles. This is the largest contribution to the modulus in **Figure 2**, but requires a filler concentration above the threshold for percolation (macroscopically extended interparticle contacts). For randomly oriented particles, this overlap concentration is given by

$$\phi^* = \frac{\pi}{4}f^{-2} \qquad [3]$$

The dependence of the storage modulus on MWCNT concentration for the polymer in **Figure 3** (upper panel) shows a change in slope at $\phi = 0.36\%$. Identifying this with the overlap concentration, eqn [3] yields $f = 15$, consistent with the aspect ratio determined from fitting eqn [2] to the viscosity of the material.

The percolated filler network is disrupted by deformation (Payne effect); displacement of the particles with increasing dynamic strain amplitude causes a substantial decrease in the storage modulus and a peak in the loss modulus. This behavior is shown in **Figure 5** for natural rubber containing various levels of N110 carbon black (Roland and Lee, 1990). Unfilled compounds do not exhibit this strain dependence of their dynamic properties. While displacement of the interaggregate contacts is the main origin of the Payne effect, detachment of bound polymer and disentanglement of chains can also be contributing factors.

Although the strain associated with breakup of the aggregate network varies with filler type and other variables, the required strain energy, calculated as the product of the stress and strain amplitudes, is constant for a given polymer. For carbon black and silica, this critical strain energy is in the range from 2–4 kJ m^{-3} (Robertson and Wang, 2005; Robertson *et al.*, 2007).

4 Mechanical Hysteresis

Mechanical hysteresis, which reduces efficiency and is responsible for heat buildup, is an important property of rubber (Roland, 2011). A prominent example is the braking performance and rolling resistance of tires, both related to mechanical energy losses. Hysteresis is observed in rubber subjected to either dynamic deformation or reversing strain histories. Since the magnitude of the strain is usually very different for these two types of deformation, the mechanisms contributing to the hysteresis can be different.
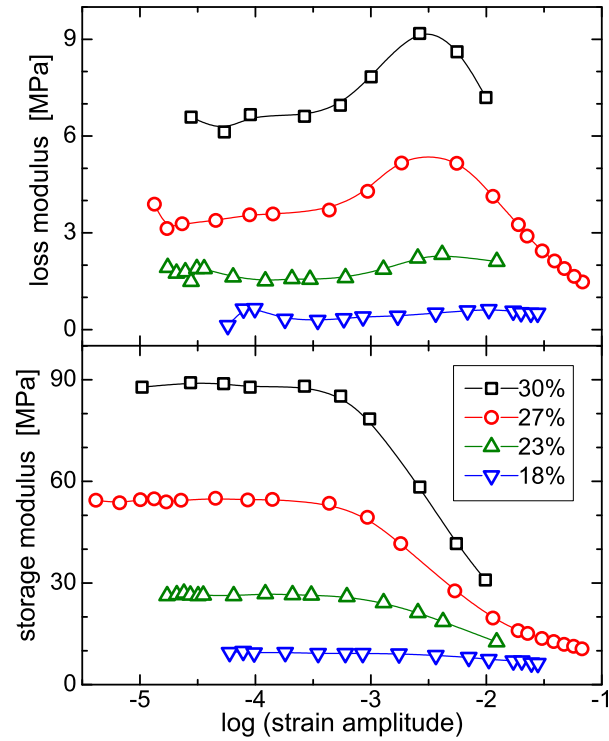
Figure 5 Payne effect in natural rubber containing the indicated amount (by volume) of N110 (SAF) carbon black (Roland and Lee, 1990).

4.1 Dynamic Properties

Under normal dynamic strain conditions, a filler-reinforced elastomer exhibits more hysteresis than its unfilled counterpart; the primary mechanism is the breakup and reformation of filler interparticle bonds. The energy loss depends not only on the mechanical properties of the compound, but is also affected by the nature of the deformation. In terms of the storage, G', and loss, G'', moduli, the energy loss for various deformation conditions is given by

$$E_{loss} = \begin{cases} = \pi\sigma_0^2\left(G''/\left[G'^2 + G''^2\right]\right) & \text{(constant stress)} \\ = \pi\varepsilon_0^2 G'' & \text{(constant strain)} \\ = \pi\varepsilon_0\sigma_0 G''/G' & \text{(constant energy)} \end{cases} \qquad [4]$$

where σ_0 and ε_0 are the respective amplitudes of the stress and strain. Complex deformations, such as that of a rolling tire, conform to none of these three conditions; however, the strain can be characterized in terms of a deformation index, n, which equals 0, 1, or 2 for constant strain, constant energy, or constant stress, respectively (Futamura, 1991). The energy loss is related to n according to

$$E_{loss} = zG''/\left(G'^2 + G''^2\right)^{n/2} \qquad [5]$$

in which z is a constant. From eqn [5] and the measured energy loss, the value of n can be determined, which via eqn [4] reveals the dynamic properties governing hysteresis for the given deformation.

Mechanical energy loss in a tire, known as rolling resistance, contributes to fuel consumption (roughly 10% for cars; at least twofold higher for trucks). However, a perfectly elastic tire would not dissipate sufficient energy to stop the vehicle during skidding. To overcome the contradictory requirements of low rolling resistance but adequate braking performance, tire treads have dissipation mechanisms only active at the high strain rates encountered during wet skidding. These generally rely on a sufficiently high glass transition temperature (> 230 K), so that the polymer segmental dynamics are on the order of 10^5 Hz or higher at ambient temperature. The energy dissipation from the Payne effect (**Figure 5**) is essentially independent of strain rate and contributes under all conditions. Thus, mixing procedures are designed to minimize the interparticle contacts and consequent network formation, in order to reduce rolling resistance without adverse effect on wet skid resistance.
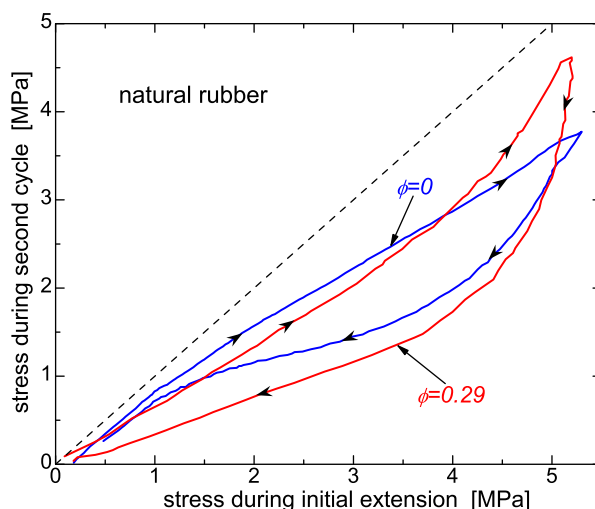
Figure 6   Stress measured during extension–retraction of natural rubber unfilled (blue line) and containing 29% by volume (80 phr) N330 carbon black (red line). The abscissa is the stress for the first extension cycle and the ordinate is the stress for subsequent cycles. The dashed line corresponds to zero hysteresis (Roland, 2011).

4.2   Strain Softening and the Mullins Effect

Uniaxial mechanical testing at a nominally constant strain rate is common in the characterization of rubber, and the effects of reinforcement are manifested in such measurements. The Young's modulus is higher due to the hydrodynamic effect and to the filler network, present. However, if the testing is carried out below the point of failure, the behavior during retraction can be observed, and this invariably exhibits large mechanical hysteresis. Known as the Mullins effect, this hysteresis is commonly assumed to be due to the filler. Actually, such softening is an inevitable consequence of polymer viscoelasticity that can be reproduced with simple spring–dashpot models. The basic mechanism is the retarded response of the polymer chains, which reduces the perturbation during retraction. The result is lower retraction stresses. Mullins softening can be reproduced in mathematical models by the use of a damping function (Roland, 2011).

In addition to this viscoelastic 'softening,' strain crystallization can cause large hysteresis during extension–retraction of rubber. Direct evidence that the Mullins effect is unrelated to filler reinforcement is the equivalent hysteresis of gum and filled rubber, when compared at similar stress levels (**Figure 6**) (Harwood *et al.*, 1965; Harwood and Payne, 1966; Roland, 2011).

5   Failure Properties of Filled Rubber

Particulate fillers improve the strength and fatigue resistance of rubber. This is illustrated in **Figure 7**, showing substantial increases in tensile strength, even for a filler such as calcium carbonate that provides minimal actual reinforcement. Similar increases in resistance to tearing and crack growth are shown in **Tables 2** (Lake, 1995) and **3** (Lake and Lindley, 1964). These improvements may seem surprising, since the hydrodynamic effect (eqns [1] and [2]) amplifies the strain of the polymer chains, and thus also amplify the local stresses. Evidently there are mechanisms that toughen the material, at least locally, to yield a net enhancement in performance. Although the topic remains to be fully understood, processes that contributed to better failure properties include strain energy dissipation from filler–polymer detachment; mitigation of stress concentration by load transfer through the particle when a chain breaks; and crack growth deviation around filler particles (Hamed, 1999; Dannenberg and Brennan, 1966; Bueche, 1958). The strength of rubber increases with filler content, attaining a broad maximum at high concentrations (Kraus, 1971).

There is a prevailing notion that the failure properties of strain-crystallizing rubbers are less affected by fillers. This is based on the idea that at the crack front, where stresses are highest and reinforcement most required, crystallites form that blunt the crack tip and toughen the material locally; thus, the need for filler reinforcement is diminished. Interestingly, although it is true that the failure properties of strain-crystallizing elastomers are generally superior to those of their amorphous counterparts, the tear, and crack growth resistance of the former still improve significantly when particulate fillers are incorporated in the compound. This is seen in the tear strength data in **Table 2**, comparing natural rubber and a non-crystallizing SBR, and **Table 3**, comparing cut growth rates for several strain-crystallizing and amorphous rubbers. Note in **Table 3**, with the exception of polychloroprene, property enhancement is greater for the higher structure filler (N330) than for the less reinforcing, thermal black (N990).

Tire wear, especially during hard braking or skidding, involves high temperatures that may preclude strain crystallization. Also, crystallization, which is not instantaneous, cannot occur at very high strain rates (exceeding c. 20 s^{-1}) (Roland, 2006). In these situations, filler reinforcement becomes mandatory, even for crystallizing rubbers, in order to achieve optimal performance. High-
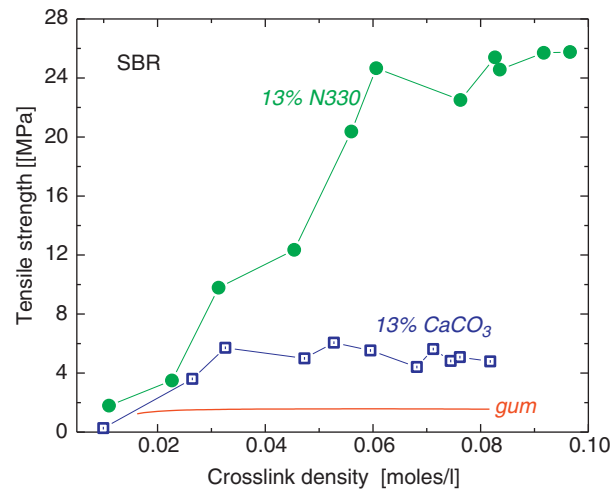
Figure 7   Tensile strength of SBR unfilled (line), with 0.13 volume fraction (45 phr) calcium carbonate (squares), and with 0.13 volume fraction (30 phr) HAF carbon black, as a function of crosslink density (Bueche, 1958).

Table 2   Effect of reinforcing filler of tear strength

Rubber	Filler	Tensile strength (MPa)	Tear test	
			Pure shear (kJ m^{-2})	Trouser tear (kJ m^{-2})
NR	Gum	28.3	6	12
	N330	28.5	12	50
SBR	Gum	2.3	1.4	3.2
	N330[a]	28.7	7	6

[a]20% by volume (52 phr).

Table 3   Effect of filler on cut growth rates

Rubber	Strain crystallize?	Carbon black[a]	Cut growth rate × 10^{-5} (mm cycle^{-1})[b]	Relative cut growth rate
NR	Yes	Gum	5.60	1
		N990	2.03	36%
		N330	0.182	0.3%
CR	Yes	Gum	25.5	1
		N990	2.71	11%
		N330	11.1	43%
IIR	Yes	Gum	97.9	1
		N990	8.89	9%
		N330	0.137	0.1%
PB	No	Gum	247	1
		N990	163	66%
		N330	1.13	0.5%
NBR	No	Gum	9.30	1
		N990	3.11	33%
		N330	0.87	9%
SBR	No	Gum	146	1
		N990	14.3	9.8%
		N330	12.1	0.6%

[a]19% by volume (50 phr).
[b]Tearing energy = 1 kJ m^{-2}.

surface area carbon blacks are considered essential for good wear. However, wear mechanisms are complicated (Veith, 1992), and since the structure and quantity of the filler affects various compound properties, there are no general principles applicable to selection of an optimal filler for abrasion resistance.

6   Summary

The majority of applications of rubber, certainly those involving mechanical properties, require reinforcement, with carbon black and precipitated silica the dominant fillers. Reinforcing fillers increase the viscosity and modulus by a hydrodynamic effect, augmented by rubber occluded within the filler. At low strain amplitude, there can be an additional contribution from an inter-particle network; breakdown and re-formation of this network during cyclic straining contributes to the hysteresis of rubber compounds. The ultimate properties (tensile strength, fatigue life, abrasive wear, etc.) are an important aspect of reinforcement, although the magnitude of the improvements and the relevant mechanisms are not always well understood. This chapter was limited mainly to conventional fillers. Nanofillers show great promise, and their commercial potential is significant. However, the dispersion problem, encountered in the use of all reinforcing fillers, remains a major obstacle to utilization of nanoparticles in the rubber industry.

Acknowledgment

References

Alateyah, A.I., Dhakal, H.N., Zhang, Z.Y., 2013. Processing, properties, and applications of polymer nanocomposites based on layer silicates: A review. Polym. Technol. 32, 21368.

Bokobza, L., 2013. Elastomeric composites based on nanospherical particles and carbon nanotubes: A comparative study. Rubber Chem. Technol. 86, 423–448.

ten Brinke, J.W., Debnath, S.C., Reuvekamp, L.A.E.M., Noordermeer, J.W.M., 2003. Mechanistic aspects of the role of coupling agents in silica–rubber composites. Comp. Sci. Technol. 63, 1165–1174.

Bueche, F., 1958. Tensile strength of filled SBR vulcanizates. J. Polym. Sci. 33, 259–271.

Casalini, R., Bogoslovov, R., Qadri, S.B., Roland., C.M., 2012. Nanofiller reinforcement of elastomeric polyurea. Polymer 53, 1282–1287.

Choi, I.S., Roland, C.M., 1996. Intrinsic defects and the failure properties of *cis*-1,4-polyisoprenes. Rubber Chem. Technol. 69, 591–599.

Dannenberg, E.M., Brennan, J.J., 1966. Strain energy as a criterion for stress softening in carbon-black-filled vulcanizates. Rubber Chem. Technol. 39, 597–608.

Donnet, J.B., Santini, A., Maafa, D., *et al.*, 2006. The difference between iodine number and nitrogen surface area determinations for carbon blacks. Rubber Chem. Technol. 79, 120–134.

Feldman, D., 2012. Elastomer nanocomposites: Preparation. Curr. Trends Polym. Sci. 16, 77–85.

Futamura, S., 1991. Deformation index – Concept for hysteretic energy-loss process. Rubber Chemistry and Technology 64 (1), 57–64.

Guth, E., 1945. Theory of filler reinforcement. J. Appl. Phys. 16, 20–25.

Hamed, G.R., 1999. The mechanism of carbon black reinforcement of SBR and NR Vulcanizates. Rubber Chem. Technol. 72, 946–959.

Harwood, J.A.C., Mullins, L., Payne, A.R., 1965. Stress softening in natural rubber vulcanizates. Part III. Carbon black-filled vulcanizates. J. Appl. Polym. Sci. 9, 311–324.

Harwood, J.A.C., Payne, A.R., 1966. Stress softening in natural rubber vulcanizates. Part IV. Unfilled vulcanizates. J. Appl. Polym. Sci. 10, 1203–1211.

Hess, W.M., McDonald, G.C., 1983. Improved particle size measurements on pigments for rubber. Rubber Chem. Technol 56, 892–917.

Kraus, G., 1971. Structure-concentration equivalence in carbon black reinforcement of elastomers. III. Application to tensile strength. J. Appl. Poly. Sci. 15, 1679–1685.

Lake, G.J., 1995. Fatigue and fracture of elastomers. Rubber Chem. Technol. 68, 435–460.

Lake, G.J., Lindley, P.B., 1964. Ozone cracking, flex cracking, and fatigue of rubber. Rubber J. 146 (11), 30–36.

Medalia, A.I., 1973. Elastic modulus of vulcanizates as related to carbon black structure. Rubber Chem. Technol. 46, 877–896.

Robertson, C.G., Bogoslovov, R.B., Roland, C.M., 2007. Effect of structural arrest on Poisson's ration in nanoreinforced elastomers. Phys. Rev. E 75, 051403.

Robertson, C.G., Lin, C.J., Bogoslovov, R.B., *et al.*, 2011. Flocculation, reinforcement, and glass transition effects in silica-filled styrene-butadiene rubber. Rubber Chem. Technol. 84, 507–519.

Robertson, C.G., Roland, C.M., 2008. Glass transition and interfacial segmental dynamics in polymer-particle composites. Rubber Chem. Technol. 81, 506–522.

Robertson, C.G., Wang, X., 2005. Isoenergetic jamming transition in particle-filled systems. Phys. Rev. Lett. 95, 075703.

Roland, C.M., 2006. Mechanical behavior of rubber at high strain rates. Rubber Chem. Technol. 79, 429–459.

Roland, C.M., 2011. Viscoelastic Behavior of Rubbery Materials. Oxford University Press.

Roland, C.M., Lee, G.F., 1990. Interaggregate interaction in filled rubber. Rubber Chem. Technol. 63, 554–566.

Sadasivuni, K.K., Ponnamma, D., Thomas, S., Grohens, Y., 2014. Evolution from graphite to graphene elastomer composites. Prog. Polym. Sci. 39, 749–780.

Shakun, A., Vuorinen, J., Hoikkanen, M., Poikelispää, M., Das, A., 2014. Hard nanodiamonds in soft rubbers: Past, present and future – A review. Composites Part A 64, 49–69.

Ulmer, J.D., Hergenrother, W.L., Lawson, D.F., 1998. Hysteresis contributions in carbon black-filled rubbers containing conventional and tin end-modified polymers. Rubber Chem. Technol. 71, 637–667.

Veith, A.G., 1992. A review of important factors affecting treadwear. Rubber Chem. Technol. 65, 601–658.

Further Reading

Dannenberg, E.M., 1982. Filler choices in the rubber industry. Rubber Chem. Technol. 55, 860–880.

Ulmer, J.D., 1996. Strain dependence of dynamic mechanical properties of carbon black-filled rubber compounds. Rubber Chem. Technol. 69, 15–47.